Thermal Model of a Thinned-Die Cooling System

N. Boiadjieva
Credence Systems Corporation,
150 Baytech Drive, San Jose, CA 95134
e-mail: nina_boiadjieva@credence.com

P. Koev
Department of Mathematics,
Massachusetts Institute of Technology,
Cambridge, MA 02139
e-mail: plamen@math.mit.edu

For through-silicon optical probing of microprocessors, the heat generated by devices with power over 100W must be dissipated [1]. To accommodate optical probing, a seemingly elaborate cooling system that controls the microprocessor temperature from 60 to 100°C for device power up to 150 W was designed [2]. The system parameters to achieve the desired thermal debug environment were cooling air temperature and air flow. A mathematical model was developed to determine both device temperature and input power. The 3D heat equation that governs the temperature distribution was simplified to a case of a 1D rod with one end at the device center and the other at the cooling air intake. Thus the cooling system was reduced to an analytical expression. From experimental data, we computed all coefficients in the model, then ran extensive tests to verify—the accuracy was better than 10% over the entire temperature and power ranges.
[DOI: 10.1115/1.1826079]

Keywords: IC Cooling, Heat Spreader, Mathematical Thermal Model, 1D Non-Uniform Rod

Introduction

Once a first silicon device is fabricated, ''real world'' validation of the design begins. About 40% of first silicon designs [3] go through this design-debug validation step. For this particular application the device under test (DUT) was in its native system level application. This method provides the unique capability of investigating devices in full system operation and using a subset of stimulus vectors to excite a certain section of the chip.

Operating at high frequencies (up to 1.3 GHz), microprocessors can consume power, up to 150 W. Even so, the internal debug of these IC devices requires removal of their heat sinks as well as thinning their silicon substrates (<100 μm remaining Si thickness). Thinning is necessary for optical probing to access individual transistor information [4]. For through-silicon optical probing of these ICs, the heat has to be removed efficiently to maintain junction temperatures at a reasonable level. This power consumption is directly related to the large number of transistors operating almost simultaneously as well as the high operational frequencies [5]. One such optical probing tool to address through silicon probing is the IDS PICA (Pico-second Imaging Circuit Analysis), which actually detects in space and time (x, y and t) the photons created when CMOS transistors switch [6] with a binning resolution of 2.5 ps and a system resolution of ~80 ps [7]. Transparent diamond enables the optical probing because it has the required transparency and the highest thermal conductivity.

Cooling a thinned microprocessor while under a functional system test on its motherboard was further complicated by space and accessibility limitations due to other motherboard components, some of which required air-cooling. A number of limitations required a compact heat spreader and heat exchanger. The optimized design needed to enable the microprocessor temperature to be regulated and maintained between 60 and 100°C as the device power went up to 150 W [2]. What is now described is the existing hardware that was designed to cool the device.

Heat Spreader and Heat Exchanger Configuration

Figure 1 shows the heat spreader/heat-exchanger arrangement that was mounted to the printed circuit motherboard [2]. The configuration consists of four basic components: (1) die-size-dependent copper heat spreader (HS); (2) heat exchanger (HE) plate with circulated cooling air; (3) pressure controlled air/thermal forcing system to provide constant air flow and (4) diamond window located between the thinned silicon die and copper heat spreader. The diamond window improved the system's thermal performance and made possible microprocessor probing by dissipating up to 150 W.

Figure 2 shows the cross section of the components interfaces. The custom device clamp was secured with 4 springs (not shown in Fig. 2). The HS had a diamond window attached to it and centered with respect to the DUT. The opening on the HS allowed the lens to move. The HE was permanently attached to the HS by 16 screws.

Heat exchanger design consisted of recirculating, concentric pathways, which expanded while flowing away from the device to facilitate thermal expansion of the forced air and to help minimize system backpressure. The pathways were made tall and narrow to accommodate the higher flow rates while minimizing the footprint of the exchanger. The thermocouples T_B and T_{HS} were used during the system test. They were the only temperature readings available during the test since there was no access to the die.

Cold air circulation into the HE was supplied by a commercially available thermal inducing system—ThermoStream TP04300A (Temptronic®). This air flow system delivered controlled temperature air from $-20°$ to $+25$°C to the HE during system functional testing. Both the air temperature and the flow rate could be controlled.

Problem Statement

Figure 3 represents a control block diagram of the thermal system [8]. We used two parameters—the temperature and flow rate of the cooling air—in order to achieve the desired thermal debug environment. Maintaining the temperature of the DUT within a certain range was critical, yet it was impossible to measure it during the full system test, and consequently we needed to derive it independently. By monitoring the system temperature at two selected locations, the T_{DUT} could be recovered using the analytical system model while the microprocessor is under a system test. The goal was to develop a mathematical model so that both the DUT temperature and input power could be derived through the analytical expression. Furthermore that expression could be used as feedback function and control the actual DUT temperature.

Manuscript received April 23, 2004; revision received June 22, 2004. Review conducted by B. Sammakia.

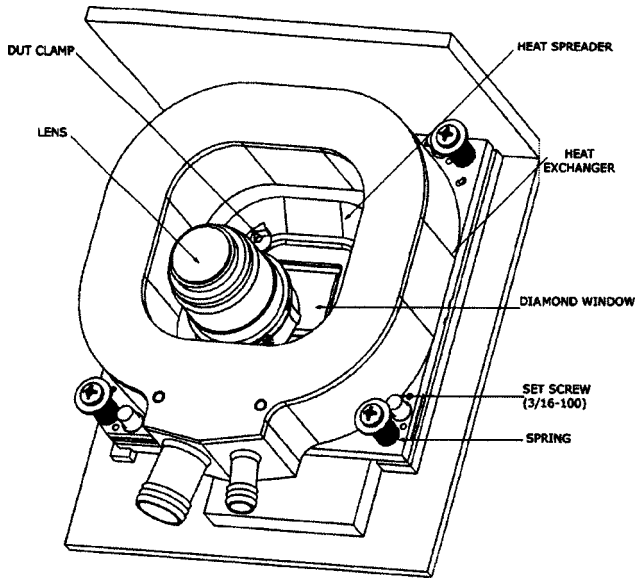

Fig. 1 Thermal system assembly

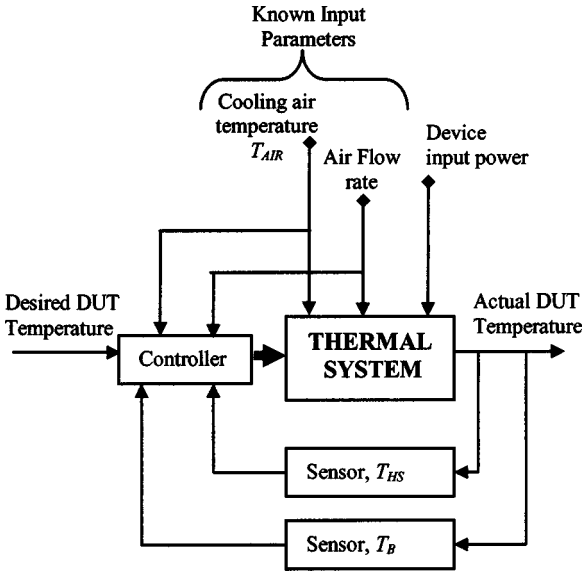

Fig. 3 Control block diagram of the thermal system

System Characterization—Thermal Test Vehicle

To characterize the system and to determine the performance of the HS and HE, a special test chip was used as a thermal test vehicle. The goal of the characterization was to determine temperature of the DUT (T_{DUT}) and input power of the device by monitoring temperature at certain locations, accessible during optical probing (Note: during design debug probing the sensor cannot be attached to the die.) Using the thermal test vehicle a thermocouple was attached onto the diamond surface and the temperature was monitored (T_{DIA}). Later those measurements were used for comparison with analytically calculated values for T_{DUT}. Figure 2 shows a half cross sectional view of system components. Three thermocouples (T_{DIA}, T_{HS}, T_B) were used for system characterization. T_{HS} and T_B were used during operational device test for thermal system control. Calculations determined that the temperature difference across the diamond window (diamond thickness was 300 μm) was ~0.08°C for 150 W power into the device and consequently we made the assumption that $T_{DUT} = T_{DIA}$.

For each air temperature, flow rate and power into the device there was a unique temperature for the HS at the measured location and for the device itself. The following represented the DUT temperature:

$$T_{DUT} = f(\text{Wattage, air } FLOW \text{ rate, cooling air temp } T_{AIR}).$$

After initial system characterization, system variable correlation was observed. Figure 4 shows the temperature of HS and diamond as a function of power into the device for a certain air temperature and air flow rate. As expected the relationship was near linear.

Figure 5 shows the relationship between cooling air temperature and HS temperature for three different airflow rates $(2.8, 4.24, 5.66)\times 10^{-3}$ m^3/s$=$(6, 9 and 12) scfm, respectively, and a constant input power of 50 W into the device.

$T_{DUT} = T_{DIA} = T_{HS} + C_1 W$ as per Fig. 4, where C_1 is a constant.

Again as expected the relationship could be approximated as a linear function.

Another parameter that can be varied in the system is the airflow. Figure 6 shows the temperature of the HS for different val-

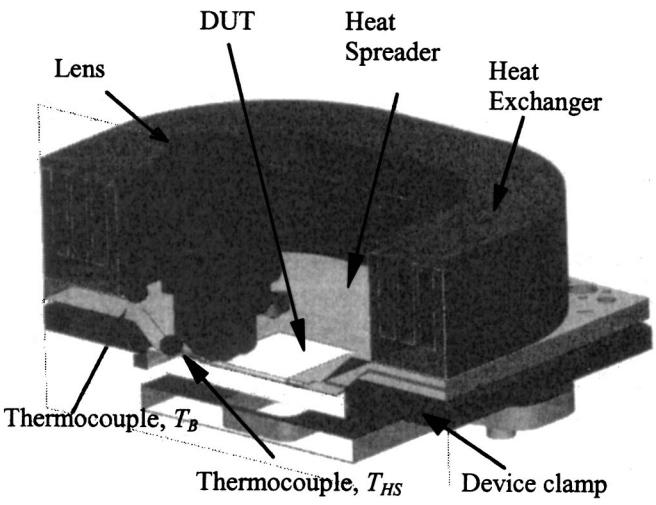

Fig. 2 Half cross section of thermal system–lens assembly

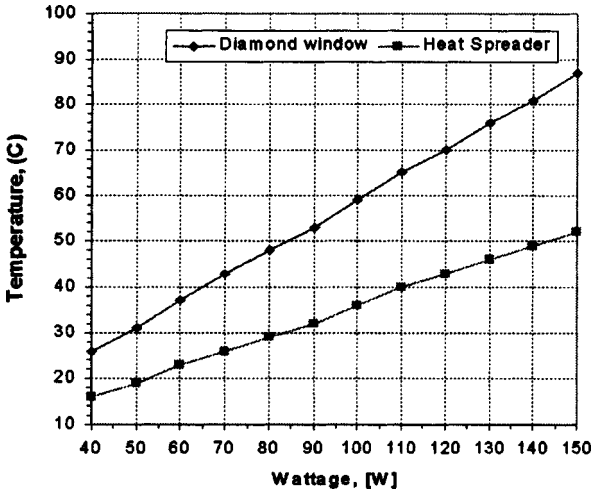

Fig. 4 Temperature variance between diamond window and HS temperature with 0°C air and (5.66×10^{-3}) m^3/s$=$(12 scfm)

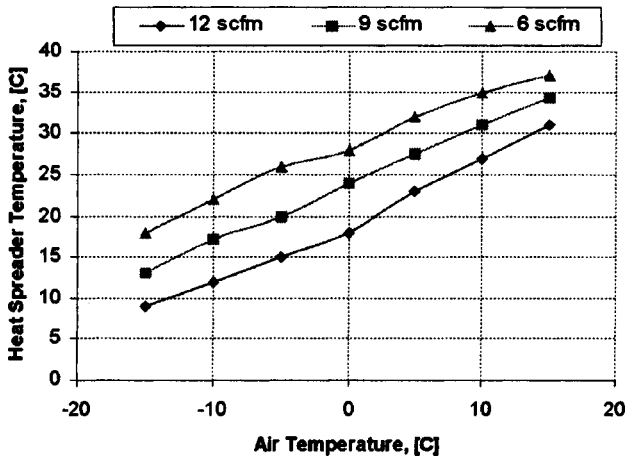

Fig. 5 Temperature of the HS as a function of air temperature for three different flow rates and constant device power of 50 W

ues of airflow. The relationship is not linear: at theoretically infinite *FLOW* the horizontal asymptote is T_{AIR} and for $FLOW=0$, the vertical asymptote is $T \rightarrow T_{DUT}$.

The system characterization was further used to determine the analytical expression coefficients. What follows is the thermal system mathematical model development.

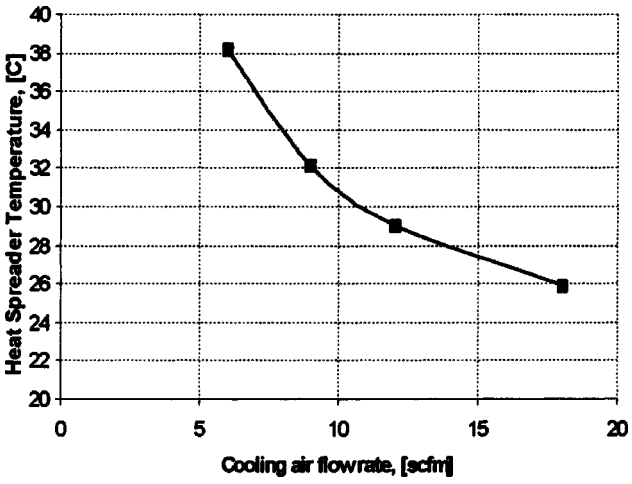

Fig. 6 Temperature of the HS for different airflow rates. The relationship here is exponential.

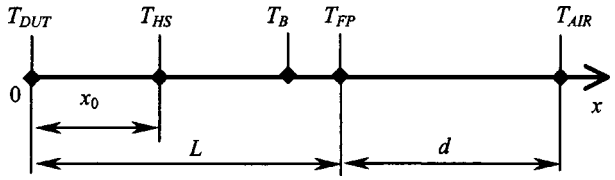

Fig. 8 System representation as 1D non-uniform rod

Mathematical Model Development

Because of the symmetry in our 3D model it suffices to study the steady state heat distribution on a 2D cross section, shown in Fig. 7. In fact, it suffices to consider the system as a 1D nonuniform rod with the cooling air on one end and the DUT on the other as shown in Fig. 8.

Here T_{DUT}, T_{HS}, T_B, T_{FP} and T_{AIR} denote the temperature on the diamond, the heat spreader, the point T_B, a hypothetical point T_{FP}, and the temperature of the air, respectively. It was convenient to identify the points T_{DUT}, T_{HS}, T_B, T_{FP}, T_{AIR} with the temperature at these points.

Our goal was to find explicit dependencies

- $T_{DUT}=f_1(W,T_{AIR},FLOW,T_{HS})$,
- $T_{DUT}=f_2(T_{HS},T_B)$,
- $W=f_3(T_{HS},T_{AIR},FLOW)$,

allowing us to compute the desired temperature or the wattage of the chip as a function of known (measurable) parameters.

We proceeded with the mathematical model.

The steady-state heat distribution $u(x)$ in a nonuniform 1D rod was governed by the well known heat equation [9]

$$\partial/\partial x[f(x)\partial u/\partial x]=0, \tag{1}$$

where $f(x)$ was the heat conductivity of the nonuniform rod $T_{DUT}T_{AIR}$ at the point x, where T_{DUT} was assumed to be at $x=0$. The only challenge was to account for the variable air flow, which could be thought of as changing the conductivity properties of a portion of the 1D rod $T_{DUT}T_{AIR}$. The airflow only affected the heat conductivity in portion of the 1D rod—$T_{FP}T_{AIR}$. The fictitious point T_{FP} was introduced artificially in this model and the temperature at this point (which was denoted by T_{FP}) only depended on the temperature of the air T_{AIR} and the air flow

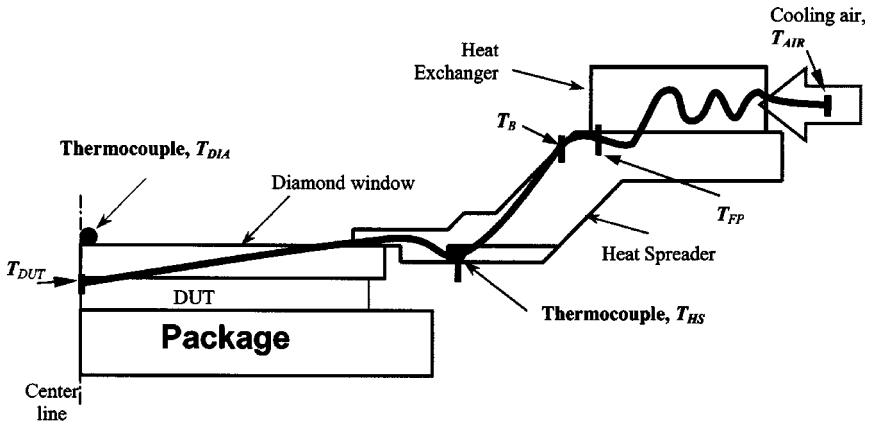

Fig. 7 Half cross section of components interface

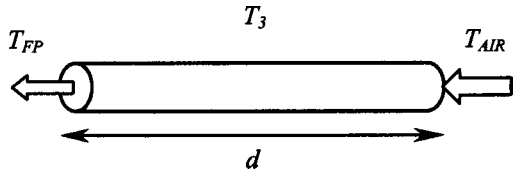

Fig. 9 System representation as 1D non-uniform rod

FLOW (and incorporates all effects of T_{AIR} and *FLOW* in the system), but was independent of the temperature on the chip T_{DUT}.

Since the thermal conductivity of $T_{DUT}T_{FP}$ was independent of T_{AIR} and *FLOW*, the temperature of the heat spreader T_{HS} would be some weighted average between T_{DUT} and T_{FP}, namely $T_{HS}=aT_{DUT}+(1-a)T_{FP}$. A similar statement was true for T_B. From (1) we obtained $du/dx=c/f(x)$ with boundary conditions $u(0)=T_{DUT}$ and $u(L)=T_{FP}$, for some constant c, where L was the distance between T_{DUT} and T_{FP}. Solving this differential equation we obtained:

$$u(x)=F(x)\frac{T_{DUT}-T_{FP}}{F(0)-F(L)}+\frac{T_{FP}F(0)-T_{DUT}F(L)}{F(0)-F(L)},$$

where $F(x)$ was such that $dF/dx=1/f(x)$. If x_0 was the distance between T_{DUT} and T_{HS} then setting $a=(F(x_0)-F(L))/(F(0)-F(L))$ we obtained the desired relationship $T_{HS}=aT_{DUT}+(1-a)T_{FP}$. By analogy $T_{HS}=bT_{DUT}+(1-b)T_B$, where b was easily recovered from experimental data to obtain

$$T_{DUT}=3.3\cdot T_{HS}-2.3\cdot T_B.$$

The dependence of T_{FP} on T_{AIR} and the air flow rate *FLOW* was more interesting. The air was released at the point T_{AIR} with initial temperature T_{AIR} and traveled a distance d before it reached the point T_{FP} at which point it had warmed up to temperature T_{FP} (Fig. 9).

Here we assumed that the air was being heated up by a constant temperature T_3, independent of T_{AIR} and *FLOW*. Since the chip was the only source of heat, T_3 would be some linear function of the wattage of the chip W and would depend on W only, i.e., $T_3=kW+s$, where k and s were constants.

Since the air was traveling at a constant rate, the distance d that the air traveled from point T_{AIR} to point T_{FP} was proportional to the time t that it took the air to travel that distance. Therefore the fact that the air was actually traveling was irrelevant, what mattered was that the air was being warmed for a specific amount of time t, proportional to d. Thus we could go a step further in our model and consider the equivalent setup of the air being a fixed 1D rod sitting in one place with initial temperature T_{AIR}, being warmed for a specific amount of time t proportional to d by a constant temperature T_3 on the boundary.

The heat equation on a 1D rod with prescribed constant temperature on both ends implied that the average temperature on the rod would decay exponentially towards the temperature on the boundary and an approximation of a form $T_{FP}=T_3+be^{-mt}$ was appropriate and reasonably accurate [9]. Here m and b were unknown constants. Since t was proportional to d and d was in turn inversely proportional to the air flow *FLOW*, it was appropriate to write $T_{FP}=T_3+be^{-h/FLOW}$, where h was also a constant. Using *FLOW* in this formula was more appropriate, since *FLOW* was our input parameter of practical interest, not d or t, which we only introduced as a part of the mathematical model. At (theoretically) infinite *FLOW* we had $T_{FP}=T_{AIR}$. Therefore $T_{FP}=T_3+b$ and $T_{FP}=kW+s+(T_{AIR}-kW-s)e^{-h/FLOW}$. Finally we obtained

$$T_{HS}=aT_{DUT}+(1-a)T_{FP}=aT_{DUT}+(1-a)[kW+s+(T_{AIR}-kW-s)e^{-h/FLOW}],$$

Table 1 A comparison between T_{DUT} obtained through the analytical model and experimental set up

Input parameters		T_{DUT} [C]	
T_{HS}	T_B	Model	Experiment
25.3	16	46.69	46
11.1	4	26.15	25
45.3	34	70.13	72

where a, k, s and h were constants. The latter were easily determined from experimental data and we could express T_{DUT} as a function of everything else to obtain the formula:

$$T_{DUT}=2.0309T_{HS}-1.0309[0.6924W+13.7825+(T_{AIR}-0.6924W-13.7825)e^{-2/FLOW}] \quad (2)$$

It was also interesting to know whether we could recover the wattage of the chip given the T_{AIR}, the flow rate *FLOW* and T_{HS}. Analogously to what we had before $T_B=b_1T_{DUT}+(1-b_1)T_{FP}$ for some constant b_1, which we recovered from experiments to obtain $b_1=0.25$, i.e., $T_{DUT}=4T_4-3T_{FP}$. Combining this with (2) and $T_{DUT}=2.0309\,T_{HS}-1.0309\,T_{FP}$ and simplifying we got

$$W=[2.9334\cdot T_B-1.4893\cdot T_{HS}-1.444(13.7825+(T_{AIR}-17.3825)e^{-2/FLOW})]/(1-e^{-2/FLOW}),$$

which allows us to compute the wattage by only knowing T_B, T_{HS}, T_{AIR} and *FLOW*.

Comparison Between Experimental Test Data and Mathematical Model Data

Table 1 shows the comparison between the T_{DUT} obtained through the analytical model and through the experimental set up. A similar comparison for wattage is given in Table 2.

From the extensive data comparison it was concluded that the accuracy was better than 10% over the entire temperature and power ranges.

Conclusions

We have described a thermal system to accommodate the through-silicon optical probing of microprocessors that generate more than 100 W.

The system was characterized and the relationships between the parameters were established. The 3D case of heat transfer was simplified to a 1D case by dividing the heat flow into two parts. The mathematical model of the thermal system was developed so that both DUT temperature and input power could be determined through an analytical expression. Having an analytical expression versus a look up table is a big advantage in terms of software control capabilities. The accuracy over the full temperature and power range was better than 10%.

Nomenclature

DUT = Device under test
FLOW = Air flow rate, [m^3/s]
HS = Heat Spreader

Table 2 A comparison between the wattage obtained through the analytical model and experimental set up

Input parameters				Wattage [W]	
T_{HS}	T_B	T_{AIR}	*FLOW*	Model	Experiment
11	4	−15	10	51.46	50
25.9	17	0	18	87	80
26.6	14	−15	12	108.9	100

HE = Heat Exchanger
T_{DUT} = Temperature of the DUT, [°C]
T_{HS} = Temperature of the Heat Spreader, [°C]
T_{AIR} = Cooling air temperature, [°C]

References

[1] Eiles, T. M., Hunt, D., and Chi, D., 2000, "Transparent Heat Spreader for Backside Optical Analysis of High Power Microprocessors," *Proc 26th ASM International Symposium for Testing and Failure Analysis*, Bellevue, WA, p. 547.

[2] Boiadjieva, N., Kelleher, C., Dajee, G., and Nadig, S., 2003, "Novel Heat Spreader for the Optical Probing of PC Board Mounted Flip Chips," *Proc 19th IEEE SEMI-THERM Symposium*, San Jose, CA.

[3] Weizman, Y., Shperber, S., and Baruch, E., 2001, "Calibration Technique for MCT FPA Used for Backside Emission," *Proc 27th ASM International Symposium for Testing and Failure Analysis*, Santa Clara, CA, p. 161.

[4] Hutcheson, D., 2002, "Climbing Reticle Costs," *The Chip Insider*™, August 15.

[5] Hecht, E., and Zajac, A., 1974, *Optics*, Addison-Wesley Publishing Company, Reading, pp. 299–300.

[6] Dajee, G., Goldblatt, N., Lundquist, T., Kasapi, S., and Wilsher, K., 2001, "Practical, Non-Invasive Optical Probing for Flip-Chip Devices," *Proc 32nd IEEE International Test Conference*, Baltimore, MD, p. 433.

[7] Goldblatt, N., Leibowitz, M., and Lo, W., 2001, "Unique and Practical IC Timing Analysis Tool Utilizing Intrinsic Photon Emission," *Proc 12th European Symposium on the Reliability of Electron Devices, Failure Physics and Analysis*, Arcachon, France, *Microelectronic Reliability*, Vol. 41, p. 1507.

[8] Ogata, K., 1997, *Modern Control Engineering*, Prentice–Hall, Upper Saddle River, NJ, Chap. 1, p. 6.

[9] Haberman, C., 1998, *Elementary Applied Partial Differential Equations*, Prentice–Hall, NJ, 3rd ed., Chap. 2, pp. 40–66.